

A reverse membrane emulsification process based on a hierarchically porous monolith for high efficiency water–oil separation†

Cite this: *J. Mater. Chem. A*, 2013, **1**, 1701

Yuchao Wang, Shengyang Tao* and Yonglin An

A hierarchically porous monolith with macro- and meso-pores was synthesized *via* a sol–gel and phase separation process. Due to the surface modification by organic silanes, the wettability of the silica material was effectively controlled. A series of hydrophobic porous silica monoliths (HPSM) were obtained. Using a “reverse membrane emulsification” process, the HPSM not only cleared oil away from water, but also broke the micro-emulsion efficiently, even when emulsion stabilizer was in the system. As the filtration layer, 1.0 g of HPSM could treat 944 mL of oil containing water or 667 mL of surfactant-stabilized micro-emulsion. HPSM materials could remove at maximum 96.5% of the oil in water and 100% surfactant in the micro-emulsion. In addition, the material could be reused through a simple treatment. The excellent separating effect was kept even after 8 times of regeneration. Special selectivity, easy operation and excellent recyclability make the material have great potential for practical application.

Received 21st August 2012
Accepted 20th November 2012

DOI: 10.1039/c2ta00007e

www.rsc.org/MaterialsA

Introduction

Surface wettability is an important property for solids, especially for porous materials.^{1–5} It can make materials themselves become hydrophobic or hydrophilic.^{6–8} This characteristic can be used to develop porous adsorbents to selectively uptake different polar or nonpolar liquids, such as water, ethanol, benzene and gasoline. Among these adsorbents, the oil-absorption materials with nonpolar surfaces are generally considered meaningful and valuable.^{9–12} For a long time, due to the exploitation, transportation and application of petroleum, oil spills have occurred worldwide, like the events in the Gulf of Mexico.^{13–15} The leaking oil causes serious environmental pollution and terrible ecological disasters, especially to the living beings in the water.¹⁶ High performance oil-adsorption materials are needed urgently.^{17–20} Meanwhile, a small amount of water in oil also needs to be separated, especially in the crude oil exploration and transmission. Surfactants are used for this purpose, however, water forms various emulsions with oil and surfactants, creating even further challenges. The droplets in these emulsions are much more stable and are difficult to separate. Chemicals are commonly added to the oil–water mixture for demulsification, but they easily cause further pollution and are difficult to clear.^{21–23} For this reason, it is

necessary to fabricate a kind of material which has a strong ability to selectively absorb the micro oil drops, catch the amphiphilic stabilizer (surfactant) and break the emulsion. Since porous membranes are widely used to produce emulsions, it is possible that the “reverse membrane emulsification” process could turn the emulsion back to the separated water and oil phase. To realize this function, first, there should be plenty of space inside the material to ensure the success of fluid flow. Additionally, the materials should be hydrophobic and oleophilic to produce high selectivity of oils against water. Finally, the surface of the material should have strong interactions with the oil molecules or surfactants in order to break the emulsion.

Hierarchically porous silica is a new kind of porous material, which has gained great attention from chemists worldwide.^{24–28} Due to the interconnected pore structure, the hierarchically porous materials have been used in catalysis,^{29–31} absorption,^{32–35} separation,^{36–38} energy storage^{39–41} and sensing.^{42–45} It was reported that the porous silica monolith could be used as a high performance column packing material in HPLC.⁴⁶ This indicates that the pore structure and surface groups may have a great effect to improve the separation property of the monolithic materials.

Herein, we report a novel kind of hydrophobic porous silica monolith (HPSM) with controlled surface wettability and hierarchical microstructure for capturing tiny oil droplets and breaking emulsions *via* a “reverse membrane emulsification” method. This material shows several advantages: first, the monolithic shape allows the silicate bulk to be used as a filtering material without further modification. Second, the

Department of Chemistry, Dalian University of Technology, Dalian, Liaoning, P. R. China. E-mail: taosy@dlut.edu.cn; Fax: +86-411-84986035; Tel: +86-411-84986035

† Electronic supplementary information (ESI) available: SEM images of HPSM, TEM images, FT-IR spectrum, TGA of HPSM and the images of the contact angles with Span 80 of the samples. See DOI: 10.1039/c2ta00007e

hydrophobic surface, covered by long-chain alkanes, could help to trap tiny oil droplet because of its high affinity to nonpolar organics. Third, the stability of porous silica allows the material to be applied in various liquid phases. Finally, facile regeneration means that the materials have a long service life and can be economically utilized.

Experimental

Materials

Tetramethoxysilane (TMOS, 99.0%) was purchased from the Chemical Factory of Wuhan University (Wuhan, China). Poly-(ethyleneoxide)-*block*-poly-(propyleneoxide)-*block*-poly-(ethyleneoxide) (P123) was obtained from Aldrich Chemical Co. Inc. Nitric acid (AR) was purchased from Beijing Chemical Reagents Factory (Beijing, China). Active carbon (AR), 25 wt% ammonia (AR), *n*-decane (AR), Span-80 (AR), toluene (AR) and petroleum ether (AR) were purchased from Fuyu Fine Chemical of Tianjin Co. Ltd (Tianjin, China). *N*-Octyltrimethoxysilane (NOEO, 96%) was obtained from Dalian Onichem Specialities Co. Ltd. *N*-Octadecyltrimethoxysilane (95%), methyltrichlorosilane (99%), phenyltriethoxysilane (98%) and (tridecafluoro-1,1,2,2-tetrahydrooctyl)-triethoxysilane (95%) were brought from Meryer Chemical Co. Ltd (Shenzhen, China).

AR stands for analytical reagent, whose purity was above 99.7%. All the reagents mentioned above were used without further purification.

Preparation of the porous silica monolith (PSM)

PSM was prepared according to the previously reported method.³⁰ First, P123 (poly-(ethyleneoxide)-*block*-poly-(propyleneoxide)-*block*-poly-(ethyleneoxide), 4.0 g) was homogeneously dissolved in an aqueous solution of nitric acid (12.0 mL of 1.0 mol dm⁻³). Subsequently TMOS (tetramethoxysilane, 5.15 g) was added and violently stirred for about 15 min for hydrolysis at 0 °C. 15 min later, the semitransparent solution was transferred into PE tubes. The PE (poly ethylene) tubes were sealed and kept at 40 °C for gelation and then aged for about 5 times the gelation time. The resultant wet gels were immersed into the 1.0 mol dm⁻³ aqueous solution of ammonia at 40 °C for solvent exchange for about 4 days. The wet silica gels were carefully evaporation-dried at 40 °C, followed by calcination from room temperature to 650 °C with a heating rate of 1 °C min⁻¹ and holding at 650 °C for 5 h in air in order to remove organic substances.

Surface modification

HPSMs were prepared due to the modification with silane coupling agents (including methyltrichlorosilane, *n*-octyltrimethoxysilane, *n*-octadecyltrimethoxysilane, phenyltriethoxysilane and (tridecafluoro-1, 1, 2, 2-tetrahydrooctyl)-triethoxysilane). PSM (1.0 g) was allowed to react with an appropriate amount of reagent (1.6 mmol) in toluene (50 mL) at reflux for 12 h. The as-prepared sample was repeatedly washed with petroleum ether and dried at 100 °C.

Preparation of the emulsion

The simple emulsion was prepared by dispersing 0.50 g of mercantile soybean oil into 1000 mL of distilled water homogeneously. The oil content in the emulsion was 0.5 g L⁻¹.

The micro-emulsion with surfactant as the stabilizer was prepared as follows: distilled water and the solution of *n*-decane with Span-80 (sorbitan monooleate) at a concentration of 0.1 wt % were mixed together at a volumetric ratio of about 1 : 9. The mixed solution was converted to homogeneous emulsion by a high-speed shear emulsifier at a shear rate of about 5000 rpm for 20 min.

Testing the effect of adsorption and separation

A block of modified silica monolith fixed on a funnel was used for the test by vacuum filtration of the emulsion. The ratio of demulsification could be obtained by measuring the volumes of the clarified water phase and oil phase. The amounts of residual oil and surfactant were tested by UV (ultraviolet) spectrometer.

Testing the density of the as-prepared materials

A block of the as-prepared material with regular shape was weighed 3 times to get the mass (*m*) and the volume (*v*) was measured by a ruler. The density of the materials (ρ) could be calculated by the following formula.

$$\rho = \frac{m}{v}$$

Characterization

The scanning electron microscopy (SEM) images were taken with a JEOL JSM-6700F field emission scanning electron microscope (FESEM, 20 kV). The transmission electron microscopy (TEM) images were taken with FEI Tecnai G² Spirit (120 kV). Mercury porosimeter (PORESIZER-9320, Micromeritics Co., USA) was used to measure the size of macropores. The nitrogen adsorption and desorption isotherms were measured at 77 K using an 3H-2000PS1/2 static volume method (Beishide Instrument-ST Co. Ltd). Samples needed to be degassed under vacuum at 373 K for 4 h before measurement. Surface areas were calculated by the Brunauer–Emmett–Teller (BET) method and the pore volume and pore size distributions were calculated using the Barrett–Joyner–Halenda (BJH) model. FT-IR spectra (4000–500 cm⁻¹) in KBr were collected on a Nicolet Avatar 360 FT-IR spectrometer. The functional materials were mixed with KBr and pressed to a thin disc for FT-IR detection. Thermal gravimetric analysis was carried out using TGA/SDTA851e coming from Mettler Co. Ltd, Switzerland. The samples were heated progressively from 25 to 800 °C at a heating rate of 10 °C min⁻¹ in air. UV spectra were obtained on a Helios Alpha UV spectrophotometer manufactured by Unicam Limited (Britain). A SL200B (Solon Tech. Inc. Ltd, Shanghai) contact-angle goniometer was used for the static contact-angle measurements. All the drops in the images were 5 μ L. The software offered by the instrument manufacturer calculates the contact angles based on the

method of the tangent. The data of Differential Scanning Calorimetry (DSC) was obtained from TA Q20 DSC (TA Instruments, USA) at a heating rate of $5\text{ }^{\circ}\text{C min}^{-1}$ and the temperature range was from room temperature to $80\text{ }^{\circ}\text{C}$ in a purified nitrogen atmosphere.

All the measurements were performed at room temperature with droplets of deionized water.

Results and discussion

Fabrication and characterization of HPSM

The hierarchically porous silica monolith (PSM in Fig. 1a) was prepared through a phase separation method at the process of sol-gel transition. The shape of the monolith depended on the container employed during the gelation of the silica sol. Plastic tubes were used to form PSM with uniform shape and the same diameter. A white silica cylinder was formed after gelation and it was easy to cut into a certain length and use for emulsion filtration. After calcination in air, the inner surface of the PSM could be fully exposed with the absence of structure directing agent. It was convenient to be modified by different organic silanes to obtain hydrophobic material (abbreviated as HPSM). The density of the HPSM was just 0.35 g cm^{-3} . And due to the hydrophobic surface formed by some alkyl groups, the monolith could flow on the water (as Fig. 1b shown). The synthesis procedure was simple, the silica sol precursor could be scaled up to 10 L in one pot and more than 1.2 kg of HPSM could be obtained at once, indicating the possibility of industrial production. The SEM images (Fig. 1c) showed that the PSM had a porous structure with interconnected porous channels. The pore diameter was nearly $3\text{ }\mu\text{m}$. After modification by *n*-octyl groups, the porous structure of HPSM-8 was kept as Fig. 1d shows. But the pore diameter (around $2.5\text{ }\mu\text{m}$) became smaller than for the unmodified ones. HPSMs modified with other silanes (see Fig. S1, ESI[†]) showed similar results. The results were in good accordance with the experimental data by the mercury intrusion method. The shrinking of the silica skeleton during the modification process might cause the decrease of the macropore diameter. The large macropore size would be a great benefit to the transfer of fluid in the porous monolith and the rough surface formed by the macroporous structure is advantageous for high hydrophobicity.^{47,48}

The mesopores inside the silica skeleton were characterized *via* TEM (Fig. S2[†]) and N_2 adsorption-desorption (Fig. 1e). The large mesopores could be observed obviously. Just as Fig. S2b[†] shows, the mesoporous structure had been kept during modification. As shown in Fig. 1e, the N_2 adsorption-desorption isotherms of the PSM and HPSMs all belong to the type-IV isotherm according to IUPAC classification.⁴⁹ It illuminated that the mesopores in the hierarchically porous system was not destroyed. As shown in Table 1, the surface area of PSM reached $377\text{ m}^2\text{ g}^{-1}$ and could still keep as $318\text{ m}^2\text{ g}^{-1}$ after *n*-octyl modification. The decrease of surface area depended on the molecular size of silane modifiers. For example, the surface area of HPSM-18 was $289\text{ m}^2\text{ g}^{-1}$, which was smaller than that of HPSM-1 ($349\text{ m}^2\text{ g}^{-1}$) and HPSM-8. The large area could enhance the contact between the surface and emulsion, which

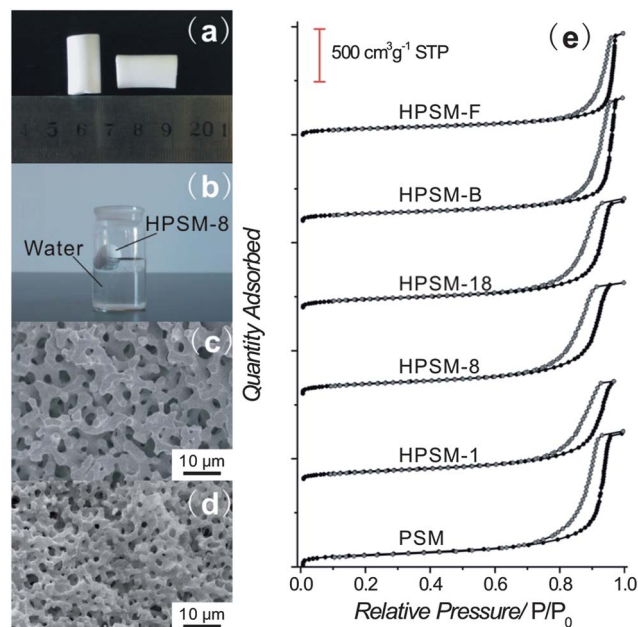


Fig. 1 (a) Optical image of the PSM. (b) The HPSM-8 in contact with water. (c) and (d) SEM images of PSM and HPSM-8, respectively. (e) N_2 adsorption-desorption isotherms.

was necessary for the breaking of emulsion. The H1-type hysteresis loops in the adsorption-desorption isotherms revealed that there were uniform mesopores with narrow pore size distribution.^{50,51} A well-defined step happened at approximately $P/P_0 = 0.85\text{--}0.96$, indicating the filling of the mesopores *via* capillary condensation. As shown in Table 1, the diameter of the mesopores in unmodified material was 17.01 nm . When *n*-octyl groups were anchored on the surface, the mesopore size decreased to 13.88 nm . The decline of pore diameter was nearly two times the length of the *n*-octyl siloxane group (about 1.45 nm), which indicated that there might be a single layer of alkyl groups on the surface. The mesopore volume was $1.64\text{ cm}^3\text{ g}^{-1}$ for HPSM-8, smaller than PSM ($1.95\text{ cm}^3\text{ g}^{-1}$), but was larger than many other reported hybrid mesoporous silica materials.^{52–56} The larger pore volume was useful for adsorbing and storing oils and surfactant molecules. The slight shrinking of the mesopores did not affect the adsorption ability of the materials since the mesopores were still large enough for the diffusion of organic molecules.

The surface properties of HPSM

According to the previous study,^{57–61} the wettability of materials depends on the surface energy and microstructure. The surface of a material with low energy and rough structure could usually get ideal hydrophobicity. According to SEM images, the porous structure of HPSM obviously provided a rough surface. The surface energy is directly bound up with the kinds of surface groups. The surface groups of HPSM were identified by the Fourier-transform infrared (FT-IR) spectrum (see Fig. S3, ESI[†]). The bands at 1082 , 2980 and 3480 cm^{-1} were assigned to the stretching vibrations of Si–O–Si, $-\text{CH}_3$ and $-\text{OH}$, respectively.⁶²

Table 1 Structural properties of the PSM and modified materials

Sample	Modifier	Dosage of modifier (mol g ⁻¹)	Macropore size (nm)	S _{BET} , specific surface area (m ² g ⁻¹)	V _p , pore volume (cm ³ g ⁻¹)	D _p , pore diameter (nm)
PSM			3.01	377	1.95	17.01
HPSM-1	Methyltrichlorosilane	1.59 × 10 ⁻³	2.51	349	1.79	14.00
HPSM-8	<i>n</i> -Octyltriethoxysilane	1.59 × 10 ⁻³	2.48	318	1.64	13.88
HPSM-18	<i>n</i> -Octadecyltrimethoxysilane	1.59 × 10 ⁻³	2.52	289	1.58	15.85
HPSM-B	Phenyltriethoxysilane	1.59 × 10 ⁻³	2.47	265	1.77	16.10
HPSM-F	(Tridecafluoro-1,1,2,2-tetrahydrooctyl)-triethoxysilane	1.59 × 10 ⁻³	2.50	227	1.45	13.75

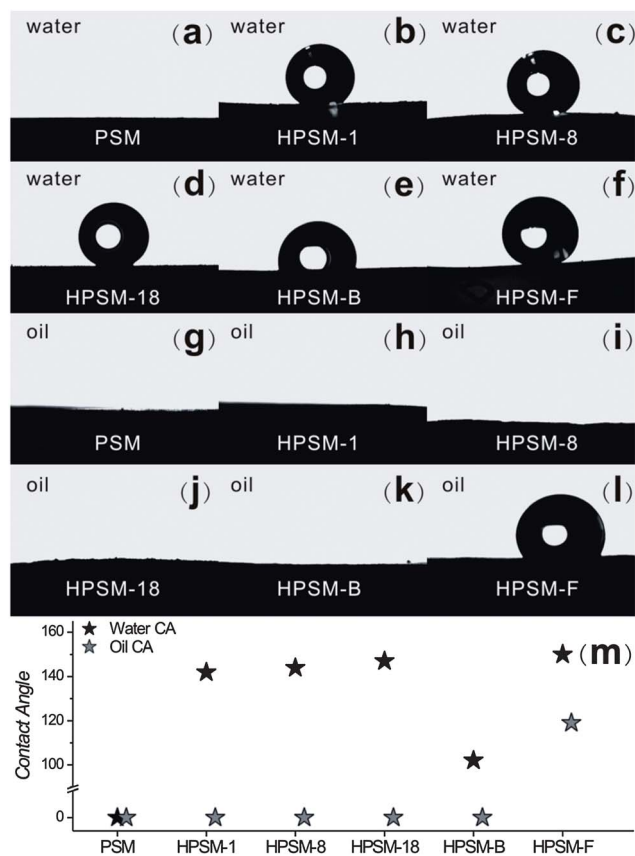


Fig. 2 The images of the water contact angles (a–f), the oil (soybean oil) contact angles (g–l) and the contact-angle data (m). The materials include PSM (a and g), HPSM-1 (b and h), HPSM-8 (c and i), HPSM-18 (d and j), HPSM-B (e and k) and HPSM-F (f and l).

When octadecyl was covered on the silica surface, the vibration strength of $-\text{CH}_3$ was distinctly enhanced. As shown in Fig. S4 (see ESI[†]), thermogravimetric analysis (TGA) was utilized to explore the coverage degree of alkyl groups on the modified surfaces. The grafted density of alkyls was about 0.8–1.1 per nm², which was calculated through the mass loss. This result provided further evidence to prove the formation of the single alkyl layer on the pore surface. The properly grafted density, which was not too low or too high, made the HPSM have both low energy surface and large pore volume.

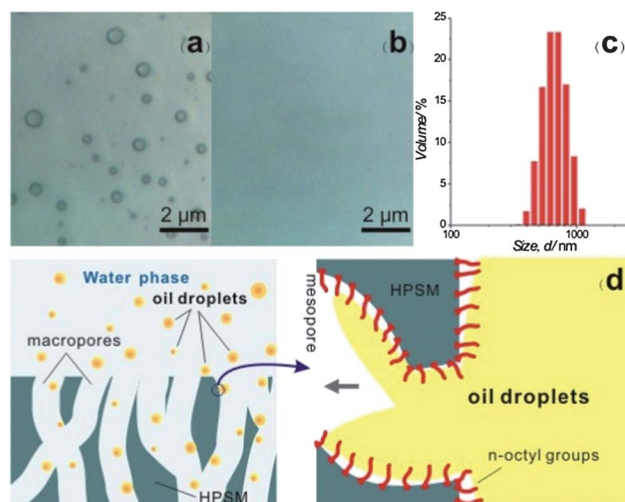


Fig. 3 The images of the emulsion before (a) and after (b) filtration by HPSM-8 and the diameter distribution of droplets in emulsion (c). A conjecture of the adsorption process of oil droplets by HPSM-8 (d).

Due to the modifications the HPSMs were expected to have ideal selectivity to oil and surfactants, the contact angles were tested to examine the surface wettability of the materials. In Fig. 2a, the water contact angle of the PSM was less than 4°, meaning that it was superhydrophilic. The abundant $-\text{OH}$ groups on the surface and the porous microstructure was believed to lead to this phenomenon. After modification, HPSM-8 became hydrophobic with the contact angle of 144° (as Fig. 2c shown). The situations were similar for HPSM-1, HPSM-18, HPSM-B and HPSM-F (Fig. 2b and d–f). Their surfaces were all hydrophobic with water contact angles between 102° and 150°. Due to the reduction of the surface energy, long-chain alkyl or fluoro-alkyl groups made the surface have better hydrophobicity. In another aspect, according to the oil contact angle (in Fig. 2g–l), all the HPSMs showed oleophilic properties (the oil contact angles were nearly 0°), except the HPSM-F. The surface of HPSM-F showed an amphiphobicity, which is usually found in fluoro-alkyl modified materials. This property meant the HPSM-F had a weak interaction with both water and oil. The results of the contact angles with the surfactant (Span-80) could be obtained from Fig. S5 (see ESI[†]). They were similar to the oil contact angles.

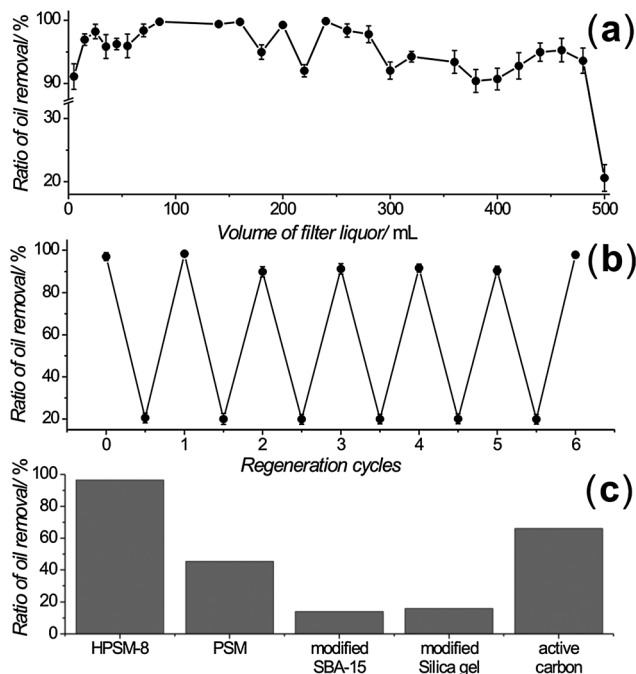


Fig. 4 The oil removal ability of HPSM-8 for 0.5 wt% (soybean oil) emulsion (a), the regeneration capacity (b) and the comparison with some other materials (c).

Removal of oil droplets from emulsion by HPSM

The separation properties of HPSM modified by different groups were explored by using them as filtration materials. A block of HPSM column with a length of 0.53 cm and diameter of

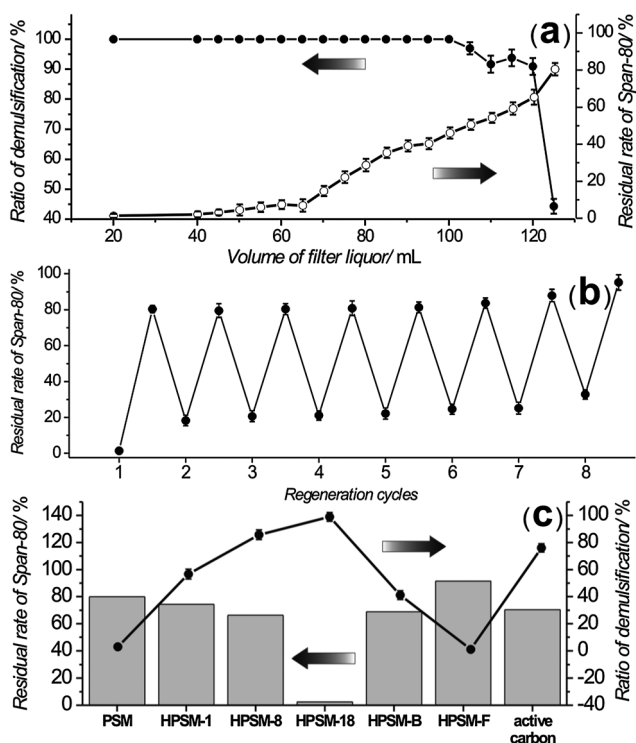


Fig. 5 The demulsification and surfactant (Span-80) removal abilities of HPSM-18 (a), the regeneration capacity (b) and the comparison with some other materials (c).

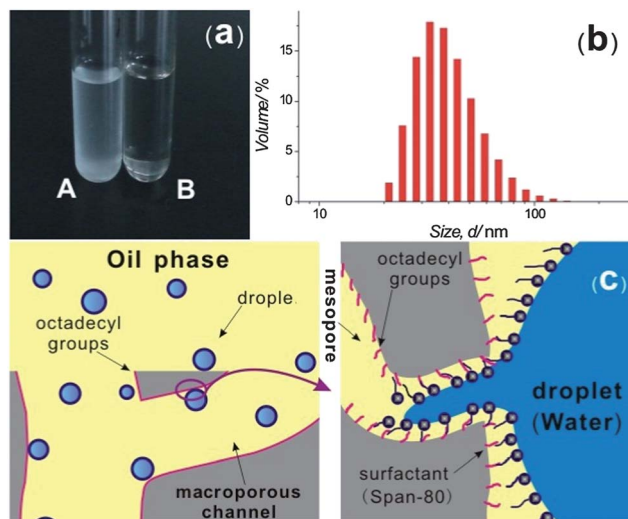


Fig. 6 (a) Image of the filtrated solution which were partly, A, and completely, B, demulsified. (b) The diameter distribution of droplets in micro-emulsion and (c) the mechanism of the demulsification by HPSM-18.

1.1 cm was sealed in the epoxy resin plaster. The upper and lower ends of the column were exposed to air and connected with plastic tube to let fluid pass through. The water-oil emulsion was filtrated through the column under vacuum. Comparing with PSM, the HPSM-8 showed an outstanding separation capacity. After filtration, the tiny oil droplets nearly disappeared in the filtrate solution, as shown in Fig. 3a and b. 500 mL emulsion (containing 0.5% oil in weight) could be treated by 0.53 g of HPSM-8. 96.5% of oil in emulsion was removed. According to the dynamic light scattering results, the average diameter of the oil droplet was 6.7 nm (Fig. 3c), much smaller than the macropore diameter of the HPSMs. When the oil droplets flowed through the macropore with water, they could easily reach the inner pore surface and be adsorbed into the mesopores (Fig. 3d).

The hydrophobic surfaces and the van der Waals forces between surface and oil molecules were thought as the main reason. Meanwhile, the large pore volume provided space to store the adsorbed oil droplets. For other hydrophobic materials, HPSM, HPSM-1 and HPSM-B showed a poor selectivity for water and oil. A great amount of water was also adsorbed. The emulsion was still very cloudy after filtration. This might be caused by the poor hydrophobicity and weak interactions between the surface and oil. The carbon chain on the surface was too short to produce enough interactions. Although HPSM-F showed a large contact angle, its surface was both hydrophobic and oleophobic. Also, it couldn't produce a selective adsorption. Compared with the HPSM-8, the HPSM-18 exhibited similar selective adsorptivity to the tiny oil droplets in the emulsion, but its adsorption capacity was smaller than that of HPSM-8. This might be due to its smallest pore volume among all the hydrophobic HPSMs, which was caused by the modification of long octadecyl groups. The adsorption capacity of HPSM-8 was also better than many popular adsorbents. SBA-15 and commercial silica gels were modified with *n*-octyl groups,

Table 2 The demulsification efficiency of some state-of-the-art materials

Material	Emulsion type	Emulsifier	Demulsification efficiency	Method	Reference
HPSM-18	W/O, 10% (v/v)	Span-80, 0.05%	99.95%	Filtration	
Polyvinylidene difluoride	O/W, 1.5 wt%		76%	Rotating disk filtration	63
Polyether modified by nano-SiO ₂	W/O, 40 wt%		96.78%	Shake	64
Polysaccharide Nanofibrous	O/W, 1350 ppm		99.5%	Filtration	65
Ethyl cellulose polymers	W/O, 5 wt%		90%	Gravity settling	66
Modified resin	O/W, 1 g L ⁻¹	SDBS ^a	80%	Filtration	67
Fibrous filter	O/W, 0.2 wt%	SDBS ^a , 5 × 10 ⁻⁵ wt%	73%	Filtration	68
ZnO nanorod array-coated mesh films	O/W, 30% (v/v)		95%	Filtration	69
Polymer membrane	W/O, 1 wt%	D2EHPA ^b , 5 wt%	98–99%	Filtration	70

^a SDBS meaning sodium dodecyl benzene sulfonate. ^b D2EHPA meaning di-2-ethylhexyl phosphoric acid.

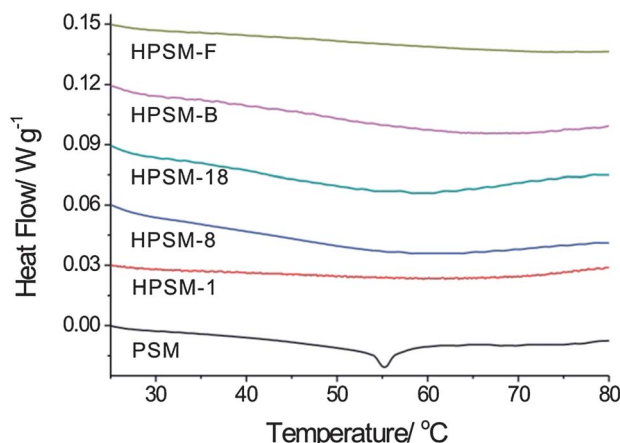


Fig. 7 Differential scanning calorimetry (DSC) of PSM and HPSMs composited with Span-80 from 25 °C to 80 °C.

but they exhibited a very low oil removal ability. As the general adsorbent widely used, active carbon didn't show a better oil removal ability than HPSM-8. The hierarchical structure and larger pore volume should greatly improve the oil-capturing capacity of HPSMs. The adsorption property of HPSM-8 could be totally recovered by organic solvent washing. After recycling 6 times the ratio of oil removal still reached nearly 100% (Fig. 4).

Demulsification of emulsions stabilized by surfactants

In addition to the simple water–oil emulsion, there are many complex emulsion systems which are stabilized by surfactants. Since lots of non-ionic surfactants are used in the petroleum industry, water is easily induced into oil during the exploitation and transmission procedure. The residual water is an important parameter to the quality of petroleum. The emulsion droplets are usually smaller than those in a simple water–oil mixture system and it is difficult to directly separate water from oil by physical filtration. Some demulsifiers can break these emulsions, but they bring secondary pollution at the same time. It is interesting that demulsification can be perfectly realized as the emulsion passes through our HPSMs.

The HPSM-18 exhibited the best demulsification ability. After the emulsion stabilized by Span-80 (a commonly used

emulsifier) was filtrated with the HPSM-18, the white emulsion turned transparent immediately. The aqueous phase and oil phase clearly separated. According to the light scattering results, the ratio of demulsification reached 99.95%. The removal of emulsifier from the emulsion was considered the main reason for the demulsification. The content of Span-80 was small in the initial filtrate and changed with the increase of the volume of filter liquor (as Fig. 5a shown). The filtration material adsorbed most of the surfactants. Lacking enough emulsifier, the emulsion became unstable and phase separation happened. When the demulsification capacity of HPSM-18 reached saturation, the residual rate of emulsifier was close to 100%. It meant that the HPSM-18 could not capture more emulsifier from the emulsion. Fig. 6a showed the filtrated emulsion. When demulsification was thorough, there was a distinct phase interface between water and oil and the solution was transparent. When the solution was halfway demulsified, the filtrated solution was cloudy and the interface was not clear.

The HPSM-18 could also be totally recyclable. After being washed by petroleum ether, the emulsifier-capturing ability of the HPSM-18 was recovered and the demulsification ability didn't show an obvious decrease after 8 cycles (Fig. 5b). Compared with the HPSM-18, other HPSMs showed a lower demulsification capacity and fewer emulsifiers were captured by them (Fig. 5c). It was surprising that the HPSM-8 didn't show a satisfied performance on non-surfactant emulsion removal. The material modified by octadecyl groups displayed a large adsorptive capacity, which was quite different from HPSMs modified by other groups. This might be due to the interactions between the octadecyl group on the silica surface and the alkyl tail in Span-80, which was an octadecanoic acid ester. The similar length of long carbon chains could produce a strong van der Waals force and hydrophobic interaction. In addition, active carbon could do well in demulsification, but couldn't removal the emulsifier (Span-80) efficiently. Comparing with many other kinds of state-of-the-art materials, HPSMs also had outstanding demulsification efficiency (Table 2). Different from the membranes, HPSMs could adsorb the emulsifier to avoid that the emulsion formed again.

Since the size of the emulsion droplets was small (35–45 nm, shown in Fig. 6b), the supposed mechanism is shown in

Fig. 6c. Firstly, the emulsifier-stabilized droplet was captured by the surface of HPSM-18. Then the micelle broke under the impact of flow. The surfactants remained on the silica surface and the droplet was released. Finally, the unprotected small droplets got together to form another continuous phase. This was just like a “reverse membrane emulsification” process. In membrane emulsification, small emulsion droplets were produced when liquid passed through the porous substrate. Pores in the membrane were used to help to form the emulsion. But for HPSM, when the surface properties were changed, droplets were forced to combine together in the porous structure and the emulsion was broken. So “reverse membrane emulsification” was employed to describe this phenomenon. The DSC results further support our conjecture. The same amount of emulsifier was adsorbed on the surface of different HPSMs, whose masses were also the same. The adsorptive layer of the emulsifier could produce an interaction with the alkyl groups on the silica surface and the intensity of this interaction related to the thermal properties of the materials. As shown in Fig. 7, endothermic peaks appeared after the emulsifier was adsorbed. For PSM, the peak was sharp and narrow. The enthalpy change was small, just 0.5 J g^{-1} . When alkyl groups were grafted on the surface, the endothermic peaks became broad, and the enthalpy change greatly increased. The enthalpy change of HPSM-18 was 3.6 J g^{-1} , and larger than that of other HPSMs, indicating that HPSM-18 had a wide and strong interaction with Span-80, which was beneficial for the demulsification process.

Conclusions

In summary, we have demonstrated a fast and efficient demulsification method with hydrophobic porous silica monolith (HPSM), based on the combination of excellent surface performance (high selective adsorption for oil and non-ion surfactant) and unique structure properties of hierarchical pores (flow passing through and storage of oil). Oil droplets in a simple emulsion system (without emulsifier) were easily removed *via* filtration. The ratio of the oils reached nearly 100% and the materials could be recycled several times. More importantly, using a “reverse membrane emulsification” process, the emulsion stabilized by surfactant could be completely broken. The long-chain hydrocarbon modified HPSM-18 exhibited the best demulsification ability *via* adsorbing the emulsifier from the emulsion. The demulsification ratio reached 99.95% and the materials also could be reused. The surface interactions between the modifier and emulsifiers was the primary driving force to remove these stabilizers from the emulsion and realize demulsification. Because of the facile preparation and high performance of the modified HPSMs in the treatment of emulsion, it could be integrated into filtration systems as a new component to separate the water–oil mixed system. In addition, the development of a monolith with different pore structure, controllable surface properties and which shows considerable adsorptivity is beneficial for the design of efficient separation materials.

Acknowledgements

We are genuinely grateful to the National Natural Science Foundation of China (20903018 and 51273030) and the Fundamental Research Funds for the Central Universities (DUT11LK23) for support of this research.

Notes and references

- 1 R. N. Wenzel, *Ind. Eng. Chem.*, 1936, **28**, 988.
- 2 A. B. D. Cassie and S. Baxter, *Trans. Faraday Soc.*, 1944, **40**, 546.
- 3 R. Blossey, *Nat. Mater.*, 2003, **2**, 301.
- 4 I. P. Parkin and R. G. Palgrave, *J. Mater. Chem.*, 2005, **15**, 1689.
- 5 T. L. Sun, L. Feng, X. F. Gao and L. Jiang, *Acc. Chem. Res.*, 2005, **38**, 644.
- 6 H. Y. Erbil, A. L. Demirel, Y. Avci and O. Mert, *Science*, 2003, **299**, 1377.
- 7 L. Feng, S. H. Li, Y. S. Li, H. J. Li, L. J. Zhang, J. Zhai, Y. L. Song, B. Q. Liu, L. Jiang and D. B. Zhu, *Adv. Mater.*, 2002, **14**, 1857.
- 8 R. Wang, K. Hashimoto, A. Fujishima, M. Chikuni, E. Kojima, A. Kitamura, M. Shimohigoshi and T. Watanabe, *Nature*, 1997, **388**, 431.
- 9 C. H. Su, *Appl. Surf. Sci.*, 2010, **256**, 2122.
- 10 J. Li, L. Shi, Y. Chen, Y. Zhang, Z. Guo, B.-L. Su and W. Liu, *J. Mater. Chem.*, 2012, **22**, 9774.
- 11 A. Marmur, *Langmuir*, 2004, **20**, 3517.
- 12 S. Y. Tao, Y. C. Wang and Y. L. An, *J. Mater. Chem.*, 2011, **21**, 11901.
- 13 Q. Wei, R. Mather, A. Fotheringham and R. Yang, *Mar. Pollut. Bull.*, 2003, **46**, 780.
- 14 D. Ceylan, S. Dogu, B. Karacik, S. D. Yakan, O. S. Okay and O. Okay, *Environ. Sci. Technol.*, 2009, **43**, 3846.
- 15 M. O. Adebajo, R. L. Frost, J. T. Klopogge, O. Carmody and S. Kokot, *J. Porous Mater.*, 2003, **10**, 159.
- 16 S. E. Allan, B. W. Smith and K. A. Anderson, *Environ. Sci. Technol.*, 2012, **46**, 2033.
- 17 J. Yuan, X. Liu, O. Akbulut, J. Hu, S. L. Suib, J. Kong and F. Stellacci, *Nat. Nanotechnol.*, 2008, **3**, 332.
- 18 X. Gui, J. Wei, K. Wang, A. Cao, H. Zhu, Y. Jia, Q. Shu and D. Wu, *Adv. Mater.*, 2010, **22**, 617.
- 19 X. Gui, Z. Zeng, A. Cao, Z. Lin, H. Zeng, R. Xiang, T. Wu, Y. Zhu and Z. Tang, *J. Mater. Chem.*, 2012, **22**, 18300.
- 20 H. W. Liang, Q. F. Guan, L. F. Chen, Z. Zhu, W. J. Zhang and S. H. Yu, *Angew. Chem., Int. Ed.*, 2012, **51**, 5101.
- 21 R. C. Little, *Environ. Sci. Technol.*, 1981, **15**, 1184.
- 22 M. A. Krawczyk, D. T. Wasan and C. Shetty, *Ind. Eng. Chem. Res.*, 1991, **30**, 367.
- 23 H. N. Abdurahman, R. M. Yunus and Z. Jemaat, *J. Appl. Sci.*, 2007, **7**, 196.
- 24 Y. Shin, J. Liu, L. Wang, Z. Nie, W. Samuels, G. Fryxell and G. Exarhos, *Angew. Chem., Int. Ed.*, 2000, **39**, 2702.
- 25 M. Hartmann, *Angew. Chem., Int. Ed.*, 2004, **43**, 5880.
- 26 D. Kuang, T. Brezesinski and B. Smarsly, *J. Am. Chem. Soc.*, 2004, **126**, 10534.

- 27 J. Smått, S. Schunk and M. Lindén, *Chem. Mater.*, 2003, **15**, 2354.
- 28 S. Hartmann, D. Brandhuber and N. Hüsing, *Acc. Chem. Res.*, 2007, **40**, 885.
- 29 A. Corma, U. Díaz, T. García, G. Sastre and A. Velty, *J. Am. Chem. Soc.*, 2010, **132**, 15011.
- 30 T. Amatani, K. Nakanishi, K. Hirao and T. Kodaira, *Chem. Mater.*, 2005, **17**, 2114.
- 31 J. Ge, T. Huynh, Y. Hu and Y. Yin, *Nano Lett.*, 2008, **8**, 931.
- 32 Q. Chen, F. Fan, D. Long, X. Liu, X. Liang, W. Qiao and L. Ling, *Ind. Eng. Chem. Res.*, 2010, **49**, 11408.
- 33 T. Ma, X. Zhang and Z. Yuan, *J. Phys. Chem. C*, 2009, **113**, 12854.
- 34 W. Cai, J. Yu and M. Jaroniec, *J. Mater. Chem.*, 2010, **20**, 4587.
- 35 G. Drisko, V. Luca, E. Sizgek, N. Scales and R. Caruso, *Langmuir*, 2009, **25**, 5286.
- 36 M. Snyder and M. Tsapatsis, *Angew. Chem., Int. Ed.*, 2007, **46**, 7560.
- 37 S. Dai, *Chem.–Eur. J.*, 2001, **7**, 763.
- 38 F. Akhtar, Q. Liu, N. Hedin and L. Bergström, *Energy Environ. Sci.*, 2012, **5**, 7664.
- 39 Y. S. Hu, P. Adelhelm, B. M. Smarsly, S. Hore, M. Antonietti and J. Maier, *Adv. Funct. Mater.*, 2007, **17**, 1873.
- 40 J. Biener, M. Stadermann, M. Suss, M. A. Worsley, M. M. Biener, K. A. Rose and T. F. Baumann, *Energy Environ. Sci.*, 2011, **4**, 656.
- 41 J. Chen, Y. Tan, C. Li, Y. Cheah, D. Luan, S. Madhavi, F. Boey, L. Archer and X. Lou, *J. Am. Chem. Soc.*, 2010, **132**, 6124.
- 42 O. Sel, S. Sallard, T. Brezesinski, J. Rathouský, D. R. Dunphy, A. Collord and B. M. Smarsly, *Adv. Funct. Mater.*, 2007, **17**, 3241.
- 43 L. C. Jia and W. P. Cai, *Adv. Funct. Mater.*, 2010, **20**, 3765.
- 44 S. Tao, J. Yin and G. Li, *J. Mater. Chem.*, 2008, **18**, 4872.
- 45 B. Fang, J. Kim, M. Kim, M. Kim and J. Yu, *Phys. Chem. Chem. Phys.*, 2009, **11**, 1380.
- 46 K. Nakanishi and N. Tanaka, *Acc. Chem. Res.*, 2007, **40**, 863.
- 47 N. A. Patankar, *Langmuir*, 2004, **20**, 7097.
- 48 M. Cathilde and D. Quere, *Soft Matter*, 2005, **1**, 55.
- 49 M. Vila, J. L. Hueso, M. Manzano, I. Izquierdo-Barba, A. Andrés, J. Sánchez-Marcos, C. Prietoc and M. Vallet-Regí, *J. Mater. Chem.*, 2009, **19**, 7745.
- 50 D. Zhao, J. Feng, Q. Huo, N. Melosh, G. H. Fredrickson, B. F. Chmelka and G. D. Stucky, *Science*, 1998, **279**, 548.
- 51 N. Nakamura, R. Takahashi, S. Sato, T. Sodesawa and S. Yoshida, *Phys. Chem. Chem. Phys.*, 2000, **2**, 4983.
- 52 C. B. Gao and S. A. Che, *Adv. Funct. Mater.*, 2010, **20**, 2750.
- 53 M. C. Burleigh, M. A. Markowitz, E. M. Wong, J. S. Lin and B. P. Gaber, *Chem. Mater.*, 2001, **13**, 4411.
- 54 W. Wang, W. Zhou and A. Sayari, *Chem. Mater.*, 2003, **15**, 4886.
- 55 B. J. Melde, B. T. Holland, C. F. Blanford and A. Stein, *Chem. Mater.*, 1999, **11**, 3302.
- 56 N. Bion, P. Ferreira, A. Valente, I. S. Goncalves and J. Rocha, *J. Mater. Chem.*, 2003, **13**, 1910.
- 57 D. Y. Ryu, K. Shin, E. Drockenmuller, C. Hawker and T. P. Russell, *Science*, 2005, **308**, 236.
- 58 J. Lahann, S. Mitragotri, T. Tran, H. Kaido, J. Sundaram, I. S. Choi, S. Hoffer, G. A. Somorjai and R. Langer, *Science*, 2003, **299**, 371.
- 59 A. Nakajima, K. Hashimoto and T. Watanabe, *Langmuir*, 2000, **16**, 7044.
- 60 K. Acatay, E. Simsek, C. Ow-Yang and Y. Z. Menceloglu, *Angew. Chem., Int. Ed.*, 2004, **43**, 5210.
- 61 L. Zhai, F. Cebeci, R. E. Cohen and M. F. Rubner, *Nano Lett.*, 2004, **4**, 1349.
- 62 N. J. Shirlcliffe, G. McHale, M. I. Newton, C. C. Perry and P. Roach, *Chem. Commun.*, 2005, 3135.
- 63 L. Li, L. Ding, Z. Tu, Y. Wan, D. Claussea and J. Lanoisellé, *J. Membr. Sci.*, 2009, **342**, 70.
- 64 F. H. Wang, L. B. Shen, H. Zhu and K. F. Han, *Pet. Sci. Technol.*, 2011, **29**, 2521.
- 65 H. Ma, C. Burger, B. S. Hsiao and B. Chu, *Biomacromolecules*, 2011, **12**, 970.
- 66 X. Feng, S. Wang, J. Hou, L. Wang, C. Cepuch, J. Masliyah and Z. Xu, *Ind. Eng. Chem. Res.*, 2011, **50**, 6347.
- 67 Y. B. Zhou, L. Chen, X. M. Hu and J. Lu, *Ind. Eng. Chem. Res.*, 2009, **48**, 1660.
- 68 S. Bansal, V. Arnim, T. Stegmaier and H. Planck, *J. Hazard. Mater.*, 2011, **19**, 45.
- 69 D. Tian, X. Zhang, Y. Tian, Y. Wu, X. Wang, J. Zhai and L. Jiang, *J. Mater. Chem.*, 2012, **22**, 19652.
- 70 N. M. Kocherginsky, C. L. Tan and W. F. Lu, *J. Membr. Sci.*, 2003, **220**, 117.